Modulation of Intrinsic Circuits by Serotonin 5-HT₃ Receptors in Developing Ferret Visual Cortex

Birgit Roerig and Lawrence C. Katz

Howard Hughes Medical Institute and Department of Neurobiology, Duke University Medical Center, Durham, North Carolina 27710

Serotonergic projections are widespread in the developing neocortex, but their functions are obscure. The effects of 5-HT₃ receptor agonists on cortical circuit response properties were studied in slices of ferret primary visual cortex using high-speed optical imaging of voltage-sensitive dye signals and whole-cell patch-clamp recording. Activation of the 5-HT₃ receptor decreased the amplitude and lateral extent of excitation throughout postnatal development. This effect peaks after eye opening, which indicates a function for serotonergic modulation of circuit responses during the period of refinement of cortical connections. Whole-cell patch-clamp recordings from single neurons revealed that synaptic responses evoked by white matter stimulation were reduced by 5-HT₃ receptor agonists, whereas the frequency of spontaneous GABAergic synaptic currents was enhanced dramatically. This indicates that the modulation of spontaneous synaptic activity by fast-acting serotonin receptors is reflected in an inhibition of the circuit response, in line with the notion of background synaptic activity altering the spatiotemporal integration properties of cortical cells by changing their membrane potential and their electrotonic structure. These mechanisms may regulate the response properties of intrinsic circuits in both the adult and developing neocortex.

Key words: neocortex; development; optical recording; serotonin; 5-HT₃ receptor; ferret; spontaneous activity; synaptic current; GABAergic synapses; inhibition

During the developmental period before the onset of sensory function, intrinsically generated spontaneous activity is crucial to the differentiation of neocortical circuitry (for review, see Goodman and Shatz, 1993; Katz and Shatz, 1996). In the visual system this activity may originate in the retina (Feller et al., 1996; Weliky and Katz, 1997), the lateral geniculate nucleus, and/or the cortex itself (Ruthazer and Stryker, 1996). Intracortical synaptic activity may also be regulated by inputs from brain regions outside the primary visual pathway.

Neuromodulatory brainstem afferents innervate the mammalian neocortex very early during development (DeLima and Singer, 1986; D'Amato et al., 1987; Gu et al., 1990; Henderson, 1991; Voigt and De Lima, 1991b). These inputs have been implicated in the regulation of ocular dominance plasticity (Kasamatsu and Pettigrew, 1976; Bear and Singer, 1986; Imamura and Kasamatsu, 1989; Gu and Singer, 1995) and the development of thalamocortical projection patterns (Cases et al., 1996), but effects on developing neocortical circuits are not well understood. The fast-acting receptors for modulatory transmitters, such as the ionotropic serotonin 5-HT₃ receptor, may structure neuronal activity in close temporal correlation with other inputs and thus play a role during activity-dependent stages of circuit formation and refinement. One function of this receptor class is modulatory: by regulating the release of GABA (Kawa, 1994), neuronal activity patterns can be altered. In addition, the 5-HT₃ receptor directly mediates fast excitatory synaptic transmission in some CNS structures (Sugita et al., 1992; Roerig and Katz, 1997). Thus serotonergic afferents to the neocortex may serve both as a source of spontaneous synaptic activity, especially in early development before the maturation of thalamocortical inputs, and as a regulator of synaptic activity mediated by other neurotransmitters.

Synaptic background activity may influence integrative properties in neocortical pyramidal cells by altering both their electrotonic structure and their resting membrane potential (Bernander et al., 1991). If neuromodulators change the frequency of synaptic background activity or the excitation/inhibition ratio, integrative properties such as coincidence detection could be significantly altered. Neuromodulators could thereby regulate spatiotemporal integration in both mature and developing circuits. To investigate whether serotonin 5-HT₃ receptors modulate cortical circuit behavior at critical stages during visual system development, we analyzed the effects of receptor selective ligands on cortical circuit response properties. Because optical recording of voltage-sensitive dye signals represents an adequate approach to measure the spatiotemporal modulation of circuit behavior (Nelson and Katz, 1995), this technique was used to monitor network level effects and single-cell patch-clamp paradigms to elucidate the underlying cellular mechanisms. We found that activation of fast, ionotropic serotonin receptors has a prominent inhibitory effect on cortical circuit responses, probably resulting from an increase in GABAergic synaptic activity.

MATERIALS AND METHODS

Animals and dissection. Postnatal ferrets (P6–P57; Marshall Farms, New Rose, NY) were deeply anesthetized with Nembutal (100 mg/kg, i.p.) and decapitated. Coronal slices (400–500 μm thickness) of primary visual cortex were prepared using a Vibratome (Ted Pella, Redding, CA). Dissections were made in sucrose–artificial CSF (ACSF) [composed of (in mM): 248 sucrose, 5 KCl, 5.3 KH₂PO₄, 1.3 MgSO₄, 3.2

$CaCl_2$, 10 dextrose, 25 $NaHCO_3$, and 1 kynurenic acid] (Aghajanian and Rasmussen, 1989) oxygenated with a mixture of 95% O_2/5% CO_2, pH 7.4, chilled to 4°C. Slices were maintained in an interface chamber at a temperature of 33°C and in an atmosphere of 95% CO_2/5% O_2 as described previously (Durack and Katz, 1996). Sucrose–ACSF was replaced with standard ACSF, composed of (in mM): 125 NaCl, 5 KCl, 5.3 KH_2PO_4, 1.3 $MgSO_4$, 3.2 $CaCl_2$, 10 dextrose, and 25 $NaHCO_3$, after 1 hr. For patch-clamp and optical recording, individual slices were transferred to a recording chamber and continuously superfused with ACSF at room temperature.

Optical recording. For optical recording of synaptic responses, the ACSF in the interface storage chamber was replaced by a 100 μM solution of the voltage-sensitive fluorescent dye RH461 (*N*-(3-trimethylammoniumpropyl)-4-(4-(*p*-diethylaminophenyl)butadienyl) pyridinium dibromide (Grinvald et al., 1987) in standard ACSF for 30–45 min. Although RH 461 was designed primarily for intracellular injection (Grinvald et al., 1987), we did not observe a difference in signal quality between RH 461 and the more expensive RH 795 (Grinvald et al., 1994) in extracellularly stained cortical slices. Individual slices were transferred to a glass-bottomed recording chamber mounted on the stage of a Zeiss IM 35 inverted microscope. Optical recordings were made using a 12 × 12 photodiode array linked to 128 sample-and-hold amplifiers (Grinvald et al., 1994). Only the 100 centermost photodiodes were used. The photodiode array was attached to the side port of the microscope, and recordings were made through a 10× objective (Wild Fluotar, 0.4 NA). The total imaged area was 1100 × 1100 mm. The preparation was illuminated by a 150 W tungsten-halogen bulb, driven at 16.5 V instead of its rated voltage of 15 V for maximum light by a stable DC power source (Kepco ATE 75, 15 M). Incident and fluorescent light was filtered using an XF40 filter set (excitation wavelength 560 nm, emission wavelength 600 nm, dichroic split at 590 nm; Omega Optical, Brattleboro, VT). The fluorescence time course was not corrected for light scattering. However, because the light scattering signal is caused by stimulus-induced activity as well, our main findings should not be affected by it even if we did not purely measure fluorescence changes induced by changes in transmembrane voltage. Slices were stimulated via a bipolar electrode (pulse duration, 100 msec; stimulation strength, 6 V; frequency, 0.04 Hz) placed at the white matter/layer 6 boundary or intracortically, usually within layer 4. To reduce fatigue of synaptic responses in young cortical tissue as well as bleaching artifacts, an intertrial interval of 25 sec was used. A total of 100 traces covering an area of 1100 × 1100 μm were recorded during each trial. To isolate the different synaptic or nonsynaptic components, the average of the last 10 trials of a recording period after addition of an antagonist were subtracted from the average of the last 10 trials of the previous condition. Receptor agonists and antagonists were bath-applied. The 5-HT$_3$ receptor agonist M-109 and serotonin were applied in the presence of the antioxidant sodium metabisulfite (100 μM $Na_2S_2O_5$), which when applied alone did not change neuronal response properties. The antioxidant was added to ensure stable serotonin and M-109 concentrations because both compounds are prone to oxidation when exposed to light. The nonspecific decrease of the optically recorded synaptic responses caused by dye washout and fatigue of synaptic terminals ("rundown") was determined by subtraction of responses recorded after 20–40 min of continuous acquisition from the responses recorded during the first 10 min of the experiment. In the slices included in this study, the time course of the nonspecific signal decline was very slow and did not show a peak during the first 20 msec of the recording, when most of the isolated synaptic responses reached their maximal amplitude. Thus we do not expect a significant contamination of our signals from this source. The amplified fluorescence signals were digitized at a sampling frequency of 2 kHz using a custom-designed Lab-VIEW Virtual Instrument. Alignment of optical recording data with laminar boundaries was guided by video images of living slices showing the area recorded from and by cresyl violet-stained sections. Overlays of fluorescence data and video images were created using Adobe Photoshop. Laminar sorting of fluorescence traces based on the position of the photodiode array was performed using a custom-designed LabVIEW Virtual Instrument. Trace data from slices of each age group were pooled according to the laminar location of the recording site, which was determined by aligning the optical traces to cresyl violet-stained sections. To compare different recording conditions, maximum amplitudes of the optical signals were integrated over the first 10 msec after stimulus onset. To correct for differences in response amplitude caused by varying distances from the stimulus position, the amplitude of the inhibitory effect (as determined by subtracting the signals recorded in the presence

of an agonist from the control condition) was plotted against the control amplitude for each trace, and the slope of the linear regression was calculated. Increasing slope values indicate larger effects (see Fig. 5). Slopes were averaged among slices for each age group.

Electrophysiology. Electrophysiological recordings were performed using standard whole-cell patch-clamp methods (Blanton et al., 1989). The intracellular solution consisted of 110 mM D-gluconic acid, 110 mM CsOH, 11 mM EGTA, 10 mM CsCl, 1 mM $MgCl_2$, 1 mM $CaCl_2$, 10 mM HEPES, 1.8 mM GTP, 3 mM ATP, pH 7.2, and contained 0.5% *N*-(2-aminoethyl)biotinamide (Neurobiotin, Molecular Probes, Eugene, OR). Unless specified otherwise, the holding potential was −60 mV. Recordings were filtered at 1 kHz, digitized at 2.5–4.0 kHz using an Axopatch 1D amplifier (Axon Instruments, Foster City, CA) and a TL-1 analog-to-digital converter in conjunction with pClamp 5.5.1 software (Axon Instruments). The frequency of spontaneous synaptic currents was determined from 1–6 min continuous recordings. Synaptic currents were electrically evoked via a bipolar stimulation electrode positioned at the layer 6/white matter border (pulse duration, 100 msec; amplitude, 130–600 mA). The slice was stimulated at a frequency of 0.1 Hz. Five to twenty-eight synaptic responses were averaged for further analysis. Slices were fixed in 4% paraformaldehyde in PBS, pH 7.4, for subsequent histological processing of neurobiotin-filled cells. Labeled cells were visualized by standard immunoperoxidase staining techniques.

RESULTS

The results of our experiments are presented in three major sections. We first analyze the composition of the voltage-sensitive dye signal to facilitate understanding of the mechanisms of the neuromodulator actions described subsequently. We then demonstrate that activation of 5-HT$_3$ receptors reduces response amplitudes and changes in the time course of optical responses. In the third section, results from patch-clamp recordings address the cellular mechanisms underlying the optically observed alterations in circuit response properties.

Components of the optically recorded signal

The optical signal integrates depolarizing and hyperpolarizing responses from a group of neurons. To be able to assign effects of serotonin receptor activation to inhibitory or excitatory, mono- or polysynaptic or action potential components, we first pharmacologically isolated synaptic and nonsynaptic components of the optically recorded response. This allowed us to understand which parts of the cortical synaptic circuitry are modulated. Figure 1 shows the pharmacologically isolated components of the optical signals recorded by a single photodiode close to the stimulation site in slices from a young (P15) and a more mature animal (P40). Maximal amplitudes of the fluorescence signal increased considerably with age. At each developmental stage the fast initial peak response was dominated by a large, TTX-sensitive component that persisted in the presence of antagonists to GABA$_A$, glutamate, serotonin, and acetylcholine receptors (antagonist concentrations used 50 μM picrotoxin, 20 μM D-APV, 50 μM CNQX, 20 nM 3-tropanyl-indole-3-carboxylate-methiodide (ICS) 205–930, 100 μM dihydro-β-erythroidine, 3 μM TTX). This potential therefore represents presynaptic action potentials. A similar contribution of presynaptic action potentials to the optically recorded signal has been observed in rat visual cortex (Tanifuji et al., 1996). The action potential component was observed close to the stimulation electrode and also at all recording sites in all layers, which differs from previous reports showing a spike contribution only in the lower part of layer 6 (Albowitz and Kuhnt, 1993; Tanifuji et al., 1996). This probably arises from differences in stimulation strength and the absence of inhibition in our experiments.

The synaptic component of the voltage-sensitive dye signal, which increased with postnatal age, was largely blocked by gluta-
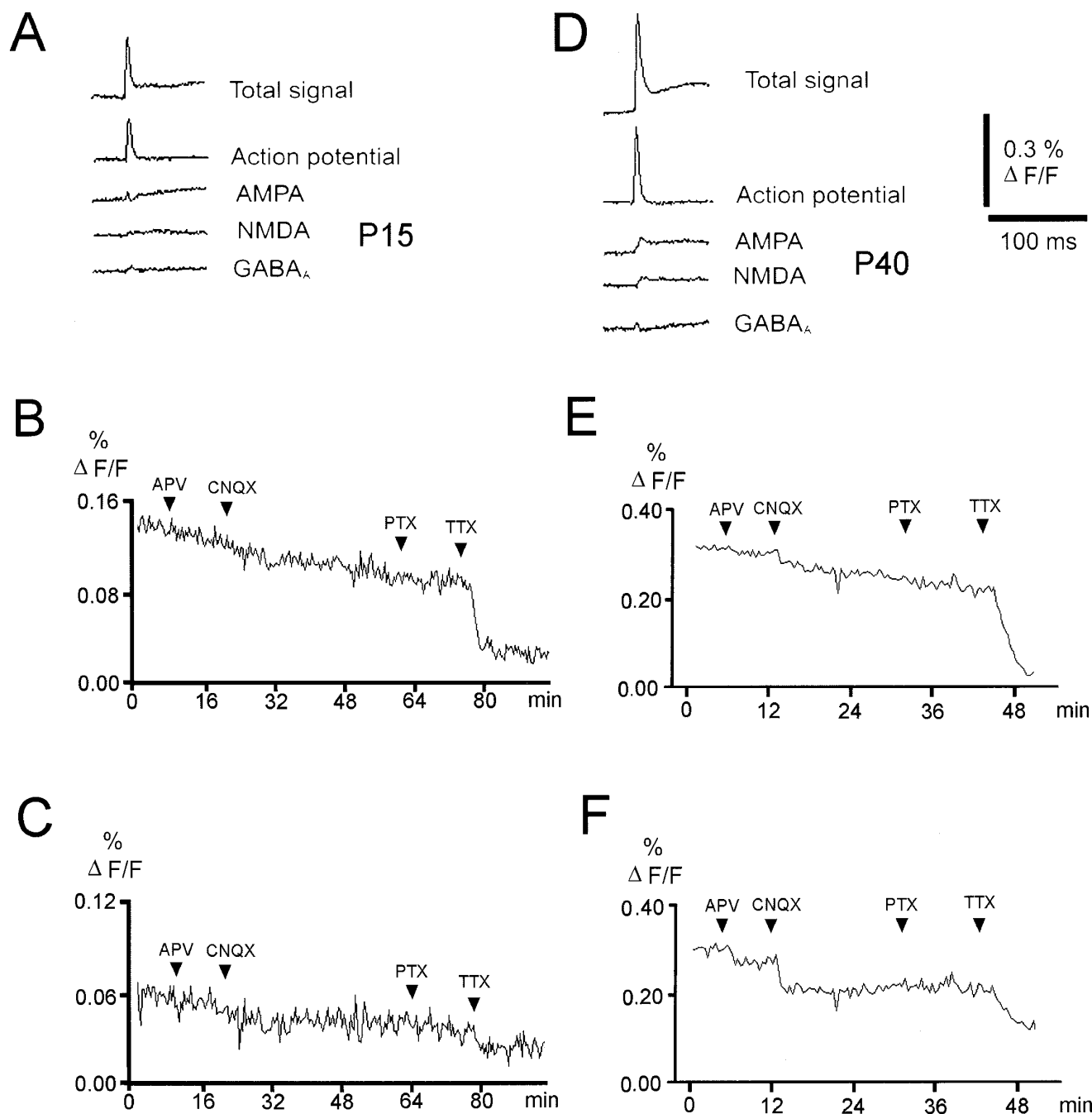
Figure 1. Pharmacologically isolated components of the optical signal. Traces represent averages of signals recorded by four adjacent photodiodes close to the stimulating electrode in slices from a young (*P15*) (*A*) and a more mature (*P40*) (*D*) animal. Upward deflections represent membrane depolarizations. All traces represent averages of 20–30 responses. Different synaptic components were isolated by sequential addition of receptor-selective antagonists and subtraction from the control condition; i.e., except for the "total signal," the traces result from subtractions. *B, C, E,* and *F* show the time course of drug-induced changes in the maximum amplitude averaged among all 100 photodiodes every 25 sec (which was the standard intertrial interval). For *B* and *E*, the first 20 msec of the signal were averaged; i.e., each point contains both the first action potential-dominated component of the optical response and the later components, which are dominated by synaptic signals. In *C* and *F*, 15 msec of the total trace starting 5 msec after the stimulus onset have been averaged; i.e., the initial spike component has been ignored to show antagonist effects on different components of the synaptically mediated response component at higher resolution. The relative contribution of synaptic components as compared with the fast, initial action potential component to the total signal increases with postnatal age. The typical response consisted of early and late glutamatergic excitatory components, occasionally separated by a $GABA_A$ receptor-mediated component, which is visible as a small hyperpolarization in a number of recordings (*D*).

mate and $GABA_A$ receptor antagonists (Fig. 1). Early and late excitatory components could be resolved in the synaptic fraction of the optical signal, presumably reflecting mono- and polysynaptic responses, respectively. The early excitatory response was dominated by an AMPA receptor-mediated component, whereas the late excitatory component was predominantly NMDA receptor-mediated. The relative contribution of NMDA and non-NMDA receptor-mediated components, however, varied consid-

erably between slices. In several slices from older animals (<35 d), an early hyperpolarizing, picrotoxin-sensitive component could be isolated close to the stimulation site, which probably reflects direct or monosynaptic activation of GABAergic interneurons. In summary, this analysis shows that the fluorescence signal roughly reflects the sequence of synaptic potentials known from intracellular recordings from neocortical neurons in response to afferent stimulation (Thompson et al., 1995). Changing the stimulus strength mostly affected response amplitudes rather than response patterns, once the threshold for action potential generation in the circuit was reached. Because changing the stimulus strength did not seem to provide us with much additional information, we have not systematically recorded at different stimulus strength in every experiment.

Activation of serotonin 5-HT$_3$ receptors reduces the amplitude of cortical responses to afferent stimulation

To investigate the effect of ionotropic serotonin receptor activation on circuit response properties, we imaged fluorescence changes in response to electrical stimulation either at the white matter/layer 6 boundary or in layer 4. At all ages (P13–P56) bath application of the selective 5-HT$_3$ receptor agonist 2-methyl-5-hydroxytryptamine maleate (100 μM M-109) reversibly reduced the amplitude of optically recorded responses in 85% of the tested slices (27 of 30) (Figs. 2, 3). Preapplication of the selective 5-HT$_3$ receptor antagonist 3-tropanyl-indole-3-carboxylate hydrochloride (10–20 nM ICS 205–930; $n = 8$) (Fig. 3*B*) blocked these effects. At all ages circuit depression by 5-HT$_3$ receptor activation was strongest when the stimulation electrode was placed in layer 4 (Fig. 3*E*). In several experiments we have observed a different laminar distribution of absolute versus relative changes in response amplitudes after application of serotonergic agonists (Figs. 2, 6). Absolute changes tended to be largest in layers 4–6, whereas relative changes seemed to be more prominent in layers 2/3. At this point we do not know whether the absolute or relative change in response amplitudes induced by serotonergic agonists is the more relevant factor in terms of its effect on the function of the cortical circuit. We have therefore restricted the representation of our results to an illustration of the absolute changes.

Analysis of isolated synaptic response components showed that activation of the 5-HT$_3$ receptor system resulted in a general reduction in cortical excitability. Cortical neurons normally generate a polysynaptic, NMDA receptor-mediated EPSP after afferent stimulation (Sutor and Hablitz, 1989). To determine the effect of 5-HT$_3$ receptor activation on the AMPA or NMDA receptor-mediated response components we tested the effects of 5-HT$_3$ receptor agonists in the presence of CNQX (50 μM) or D-APV (20 μM). Bath application of D-APV (20 μM) reduced both early and late excitatory components of the voltage-sensitive dye signal, consistent with a contribution of NMDA receptors to both mono- and polysynaptic response components ($n = 4$ slices). The 5-HT$_3$ receptor agonist M-109 strongly suppressed the remaining AMPA receptor-mediated response component.

CNQX (50 μM) reduced the early excitatory component, whereas the late, slower excitatory component was unaffected or even increased ($n = 5$ slices) (Fig. 4). Blocking the AMPA component of the early, excitatory response often revealed an early inhibitory component (Fig. 4*B*). This was most prominent close to the stimulating electrode and probably represents direct depolarization or monosynaptic activation of local interneurons. M-109 reduced both the early hyperpolarizing component and the NMDA component of the optically recorded response. The

results of these experiments demonstrate that 5-HT$_3$ receptor activation reduces both mono- and polysynaptic NMDA and AMPA components and even the GABAergic, hyperpolarizing component of the electrically evoked response (Fig. 4). This suggests a general inhibitory mechanism rather than a selective effect on any receptor subsystem.

The inhibitory effect of 5-HT$_3$ receptor activation had no obvious laminar specificity at any age. To test for developmental changes in the magnitude of the modulatory effect, data from all layers were pooled for each age group (Fig. 5). Layer 1 responses were omitted because of their small amplitude and the resulting low signal-to-noise ratio. The inhibitory action of the 5-HT$_3$ receptor agonist M-109 increased significantly between P35 and P40, i.e., during the period immediately after eye opening ($p < 0.001$; one-way ANOVA) (Fig. 5).

Effects of serotonin and 5-HT1B receptor ligands on voltage-sensitive dye signals

Serotonin activates not only 5-HT$_3$ receptors but also G-protein-coupled receptors, which themselves might alter responses. We thus next tested the effects of serotonin itself. Bath application of serotonin (100 μM) reversibly suppressed responses to afferent stimulation at the layer 6/white matter boundary in 60% of the tested slices (7 of 12, P29–P34) (Figs. 6, 7). In the remaining slices serotonin had no effect. The inhibitory effect was partially blocked (60–70%) by the 5-HT$_3$ receptor antagonist ICS 205–930 (20 nM) in all tested slices ($n = 4$). Thus a significant proportion of the effect of serotonin on circuit response properties is mediated by the 5-HT$_3$ receptor system.

A presynaptic inhibitory effect of serotonin on both thalamocortical and intracortical synaptic transmission mediated by the G-protein-coupled 5-HT1B receptor has previously been described in rat cortical slices (Read et al., 1994; Rhoades et al., 1994). To test whether this second, presumably slower acting inhibitory system also operates in the ferret cortex we used the selective 5-HT1B receptor agonist CGS-12066A (100 μM). 5-HT1B receptor activation slightly reduced response amplitudes in one of eight tested slices, had no effect in two slices, and enhanced the early peak response, whereas it depressed the late excitatory component in six of nine tested slices (Fig. 7) (age of animals P29–P35). The agonist had no effect on the presence of the 5-HT1 receptor antagonist methiotepin (10 μM). Thus the 5-HT$_3$ and 5-HT1B receptor systems do not simply represent two inhibitory mechanisms acting on a different time scale, as we initially expected, but show a more complex pattern of effects on circuit activation.

Serotonergic agonists change the time course of cortical circuit activation

The results presented thus far demonstrated that the 5-HT$_3$ receptor agonist M-109 (100 μM) reduced peak amplitudes of the optically recorded cortical response to afferent stimulation. Because the integration of subcortical and intracortical inputs also depends on the time course of signal propagation, we next compared the temporal properties of the circuit response under control conditions and in the presence of the agonist (Fig. 8). In most cases (23 of 30 tested slices) the time to response peak was unchanged or slightly faster (0.89 $\pm$ SD; 0.35 msec; $n = 23$) compared with control conditions (Fig. 8*A,B*). The signal decay, however, was considerably prolonged (2.8 $\pm$ 0.4 msec; $n = 23$) throughout all age groups (Fig. 8*A,B*). This effect was more prominent when the cortex was stimulated in
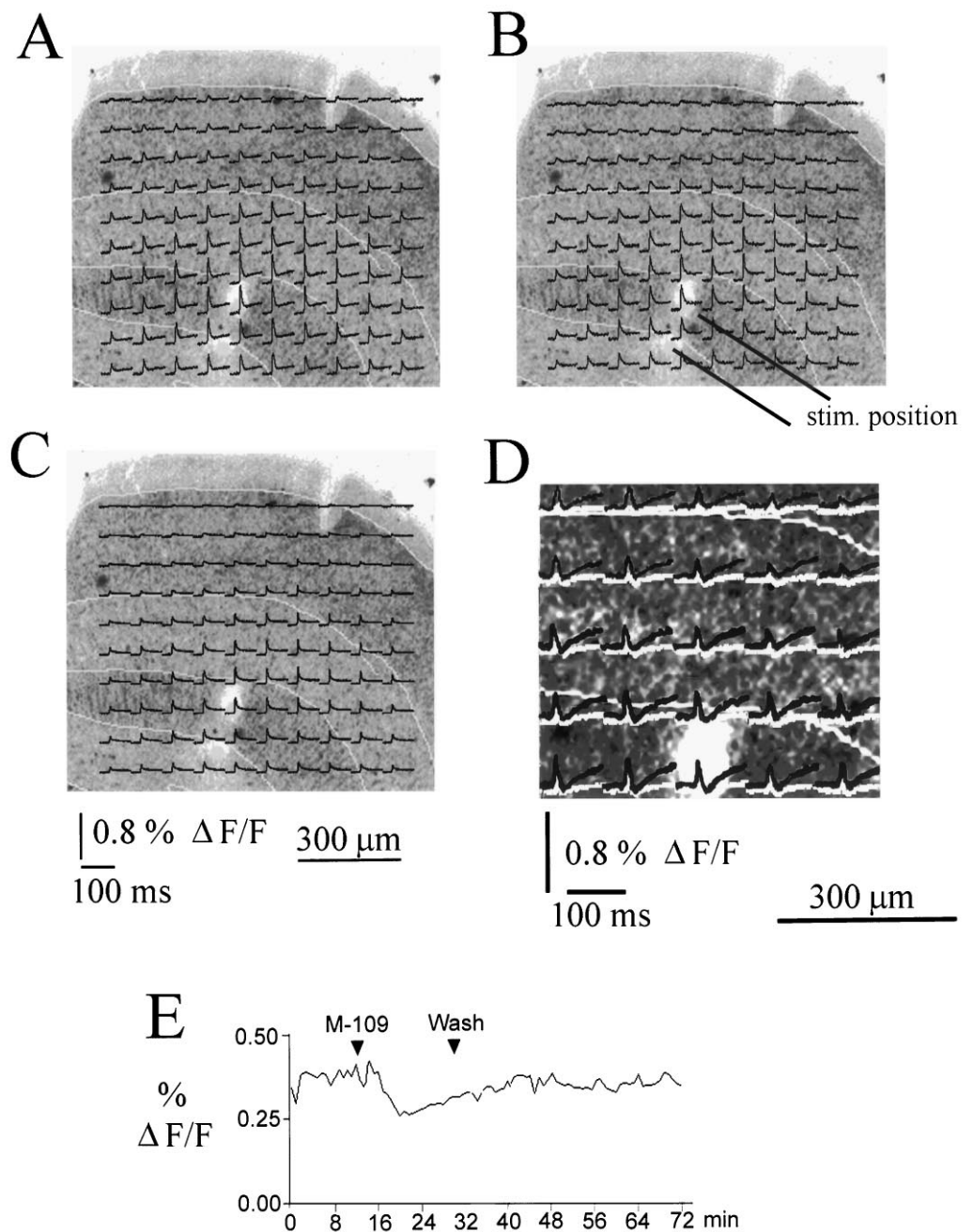
Figure 2. Reduction of response amplitudes after application of the 5-HT$_3$ receptor ligand M-109. *A–D,* Optically recorded traces overlaid on a Nissl-stained section from a P34 animal. Laminar boundaries are indicated by *yellow lines.* All traces represent averages of 20 stimulations. M-109 reduced the response amplitude in all layers. *D* shows the difference between the control response and the response recorded in the presence of M-109 (*red traces*) and the difference between control and recovery (*green traces*) at expanded vertical scale for a selection of traces close to the stimulation site. The difference between control responses and responses recorded in the presence of M-109 is clearly larger than the difference between control and recovery traces, demonstrating that the inhibitory effect of 5-HT$_3$ receptor activation is clearly distinct from rundown. *E* shows the time course of the maximum amplitude of the optically recorded response (averaged over all 100 photodiodes and the first 20 msec after stimulus onset) for the entire duration of the experiment. The reduction of the response amplitude induced by M-109 and the reversibility of the effect are clearly shown.

layer 4 as compared with layer 6 (Fig. 8*B*). The time course effects can probably be explained by a reduced and slower activation of polysynaptic connections under conditions of enhanced intracortical inhibition. A similar alteration of the time course of the cortical response was observed in the presence of serotonin, but the effect was less prominent (2.2 ± 0.86 msec prolongation of signal decay; $n = 4$). The 5-HT1B agonist CGS-12066A, on the other hand, accelerated both rise and decay of the circuit response (data not shown). Thus stimulation of different serotonin receptors differentially modulates the time course of intracortical activation.

Enhanced GABAergic activity keeps the average membrane potential of cortical neurons at more hyperpolarized levels, thereby raising the threshold for action potential generation. This should result in a lower probability for polysynaptic activation

and thus in a spatial sharpening of the circuit response. In 56% of the tested slices (15 of 27), a comparison of normalized maximum amplitude plots showed that 5-HT$_3$ receptor activation reduced both the activation of the upper cortical layers and the intralaminar lateral spread of excitation after stimulation of the white matter or lower layer 4 (Fig. 8*E,F*). Figure 8*E,F* show intrinsically normalized plots; i.e., the amplitude information is discarded to isolate temporal and spatial changes in the circuit response after M-109 application. The spatial focusing is therefore real and does not simply reflect a reduction in response amplitude. The reason for the spatial focusing being present in only 56% of the tested slices might be attributable to the variability in the magnitude of the M-109 effect in general. The increase in inhibitory activity might not always be sufficient to spatially restrict the responsive area. Because we did not vary considerably the stimulation
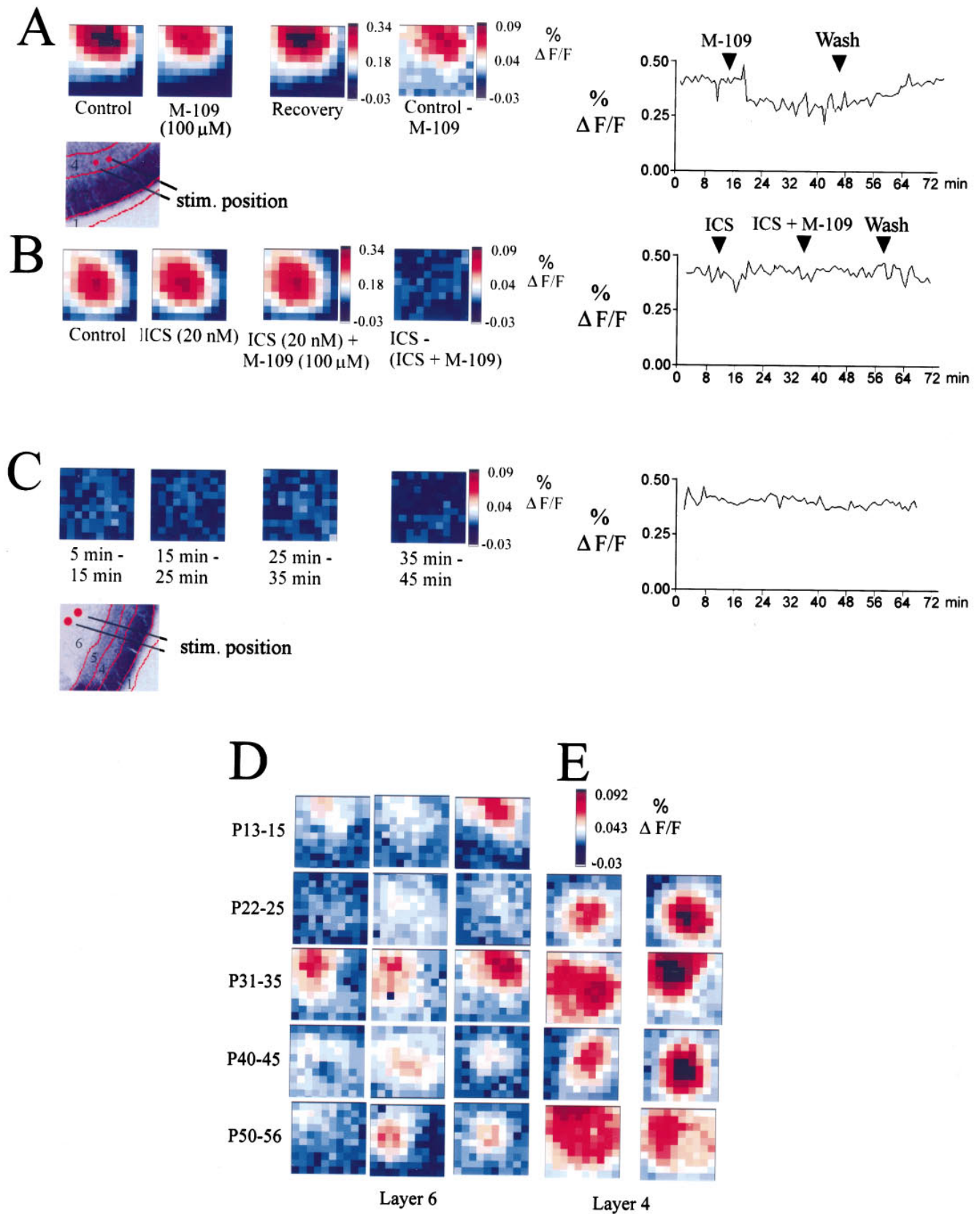
Figure 3. The effect of M-109 is reversible and blocked by the 5-HT$_3$ receptor antagonist ICS 205–930. *A–E,* Maximum response maps recorded from coronal slices. *A,* Maximum amplitude plots from another P35 slice showing the reversibility of the inhibitory effect of 5-HT$_3$ receptor stimulation. Shown are recordings from a P35 animal; the stimulation electrode was placed in layer 4 (see illustration of stimulation electrode position and laminar boundaries in *bottom panel*). The last maximum amplitude in the *top row* shows the difference between the control map and the responses recorded in the presence of M-109. The *last panel* in the *top row* shows the time course of the maximum amplitude of the averaged response during (*Figure legend continues*)
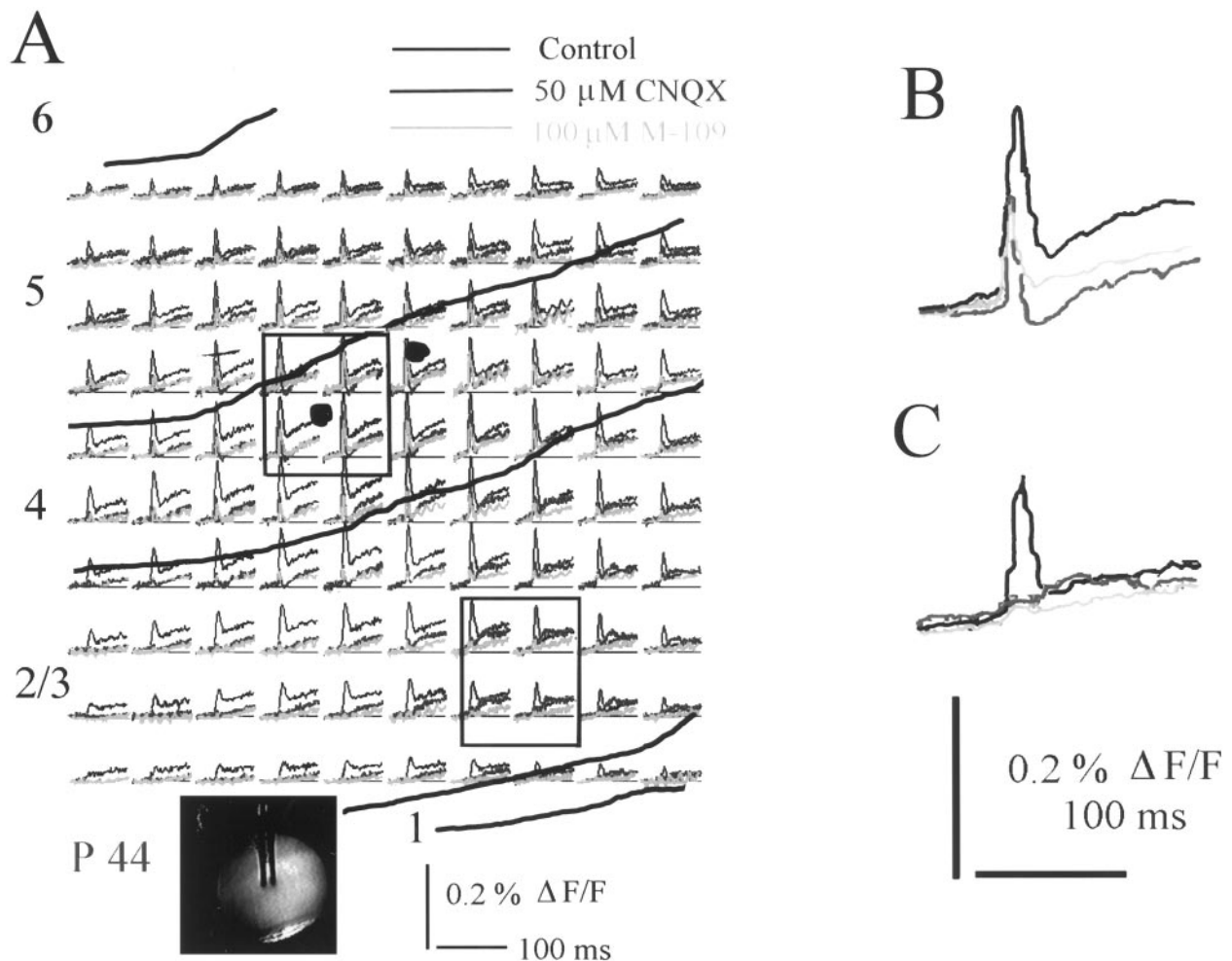
Figure 4. Effects of the 5-HT$_3$ receptor agonist M-109 after blockade of the fast, non-NMDA receptor-mediated excitatory response component. *A,* Optically recorded traces from a P46 ferret under control conditions (*white*), in the presence of CNQX (*blue*), and in the presence of CNQX and M-109 (*pink*). *Yellow lines* indicate laminar boundaries as reconstructed from cresyl violet-stained sections. The *inset* shows a video image of the living slice with the stimulation electrode. *B,* Averaged signal recorded by four photodiodes close to the stimulation site show a distinct hyperpolarizing component (*blue trace*) in the presence of CNQX. 5-HT$_3$ receptor activation reduces both excitatory and inhibitory components of the optical signal (*pink trace*). *C,* Average of four responses recorded by photodiodes more distal from the stimulation site in the supragranular layers. The late excitatory component seems enhanced in the presence of CNQX. M-109 again reduces all components of the optical signal.

strength between slices of one age group, we can exclude the possibility that the spatial focusing effect is the result of responses representing different points on the stimulus saturation curve.

Cellular mechanisms of 5-HT$_3$ receptor activation

The experiments outlined above demonstrate that activation of serotonin 5-HT$_3$ receptors results in a net suppression of circuit activation after electrical stimulation. On a cellular level the underlying mechanism appears to be an increase in GABAergic network activity. To analyze this modulatory property of the

serotonergic system, single-cell patch-clamp recordings were made in slices from animals aged between P21 and P43. A physiological chloride gradient was used to distinguish between excitatory (recorded at −60 mV) and inhibitory (recorded at −20 or 0 mV) synaptic currents. The strength of electrical stimulation was chosen to match the optical recording data, and the stimulation electrode was positioned at the layer 6/white matter boundary.

Activation of 5-HT$_3$ receptors by bath application of M-109

←

agonist application and washout. *B,* ICS (20 nM) alone had no significant effect on cortical response properties. After preapplication of ICS for 5–10 min, the effect of the 5-HT$_3$ receptor agonist M-109 (100 μM) was completely blocked. *C,* To estimate the rundown of the optical signal during a typical experimental period, we have subtracted control responses obtained at different times from each other, as indicated below the individual panels in *C.* Recordings have been made from another P35 slice. The difference plots show that no significant rundown of the maximum signal amplitude contributes to the effects described above during a normal recording period of 30–50 min. *D, E,* Examples of maximum amplitude maps showing the difference between control recordings and recordings made in the presence of M-109 (see *A, last panel*) at different ages and different positions of the stimulation electrode. *D* shows difference plots from three different slices for each of the five age groups indicated on the *left* (P13–P15 to P50–P56). Each slice in *D* has been stimulated in layer 6. *E* shows examples of difference plots for two slices for each of the four age groups, P22–P25 to P50–P56. Each slice in *E* has been stimulated in layer 4. The inhibitory action of the 5-HT$_3$ receptor agonist was usually stronger when the stimulation electrode was placed in layer 4 (*E*) as compared with the layer 6/white matter boundary (*D*).
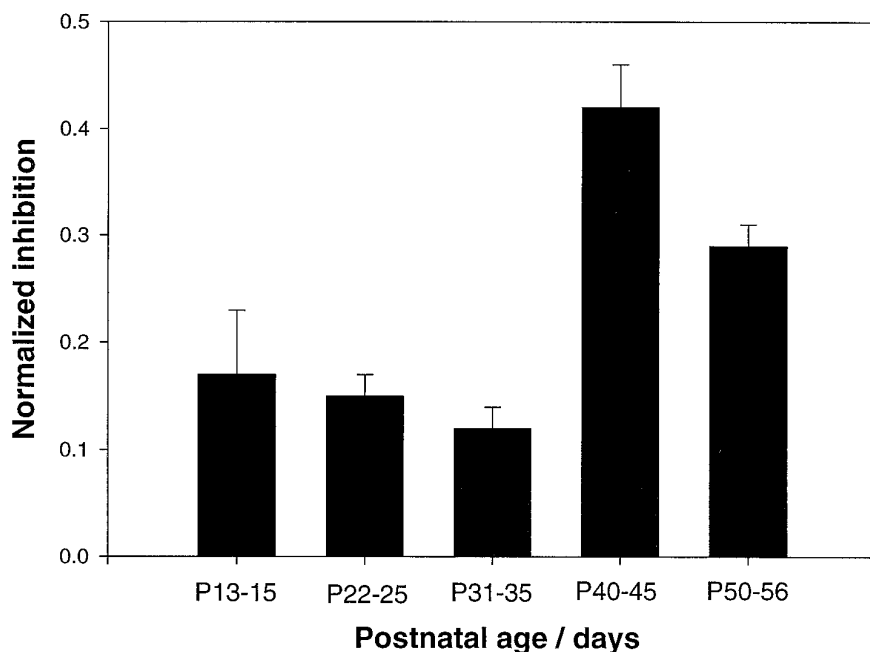
Figure 5. Developmental changes in the amplitude reduction of cortical responses after 5-HT$_3$ receptor activation. The *bar graph* shows the slopes of linear fits to effect amplitudes (i.e., maximum amplitude under control conditions − maximum amplitude in the presence of agonist) plotted against control amplitudes for each trace to normalize for different control maximum amplitude values across slices ("normalized inhibition"). This value has been derived for each of the 100 positions recorded in each slice individually; therefore the *n* represents traces, not slices. Error bars represent mean values ± SEM. Recordings obtained from layers 2/3 to 6 in different slices have been pooled according to age. Data were obtained from five to eight individual slices per age group. Each *bar* represents the average of 480–660 data points. A significant increase in the inhibitory effect occurred between P35 and P40.

(100 μM) significantly ($p < 0.05$; paired *t* test) reduced the peak amplitude of evoked EPSCs by 58.5% ± 8.1% ($n = 8$) (Fig. 9*A*). Evoked IPSCs were also significantly reduced by 53.3% ± 3.4% ($p < 012$; paired *t* test; $n = 5$) (Fig. 9*C*). Preapplication of the 5-HT$_3$ receptor antagonist ICS 205–930 (10–20 nM; $n = 7$) prevented these effects (Fig. 9*B,D*). Our cell sample included layers 2/3 pyramidal cells ($n = 9$), layer 5 pyramidal cells ($n = 5$), layer 6 pyramidal neurons ($n = 3$), and layer 4 spiny stellate cells ($n = 4$) and aspiny stellate cells ($n = 1$). The single-cell data support the results from the optical recording experiments: 5-HT$_3$ receptor activation depresses synaptic responses evoked by electrical stimulation.

An inhibition of a circuit response can be generated by various cellular mechanisms. Because the 5-HT$_3$ receptor regulates GABA release from hippocampal interneurons (Kawa, 1994), we next examined the effects of 5-HT$_3$ receptor agonists on the frequencies of spontaneous synaptic currents. Under control conditions, the mean frequency of spontaneous outward synaptic currents recorded at −20 mV was 10.1 Hz ± 1.2 Hz ($n = 16$). In half of the cells tested ($n = 16$), M-109 (100 μM) induced a large increase in the frequency of spontaneous postsynaptic currents (PSCs) ($p < 0.001$; paired *t* test; mean 220.8% ± 56.7%; $n = 8$) (Fig. 10). These events reversed near −30 mV and were abolished by picrotoxin (50 μM) or bicuculline (20–50 μM) (Fig. 10). An increase in the frequency of glutamatergic events or both glutamatergic and GABAergic PSCs was observed in only one cell each. The increased GABAergic synaptic activity was completely suppressed by preapplication of ICS 205–930 ($n = 6$). The 5-HT$_3$ receptor-induced increase in synaptic activity was reversible but lasted for at least 3–5 min and in some cases for >20 min (mean 12.4 ± 7.8 min; $n = 8$).

To determine whether the increase in spontaneous synaptic activity induced by 5-HT$_3$ receptor agonists involved presynaptic regulation of transmitter release or mainly represented action potential-evoked activity, we applied M-109 (100 μM) in the presence of TTX (3 μM). Under this condition no increase in the frequency of spontaneous GABAergic events was observed ($n = 13$). Thus the increase in excitability of the GABAergic network

by activation of serotonin 5-HT$_3$ receptors requires action potential activity, presumably in interneurons. A recent study has shown that 5-HT$_3$ receptors are expressed by different subpopulations of GABAergic neurons, including cholecystokinin-, calbindin-, and calretinin-containing cells in rat cortex (Morales and Bloom, 1997).

The single-cell data presented above argue strongly in favor of a GABAergic mechanism underlying serotonergic suppression of cortical circuit responses. We next tested whether GABA$_B$ receptors might contribute to these effects. Preapplication of the GABA$_B$ receptor antagonist 2-OH-saclophen (300 μM) antagonized the inhibition of optically recorded circuit activation induced by 5-HT$_3$ receptor stimulation (30–80%; $n = 6$ slices) (Fig. 11). This indicates a contribution of GABA$_B$ receptor-mediated inhibition in addition to the GABA$_A$ receptor-mediated effects.

To test whether the effects of external agonist application were not altered by RH 461, we made single-cell patch-clamp recordings in dye-stained slices and filled the recorded cells with neurobiotin. In this preparation 5-HT$_3$ receptor activation still enhanced GABAergic synaptic activity in 54.5% of the tested cells (mean frequency increase 180 ± 67%; $n = 6$), comparable to the effect in unstained slices. The recorded cells (nine pyramidal cells and two spiny stellate cells) also showed normal morphology.

DISCUSSION

The serotonergic projection is a major modulatory input system to the neocortex. By regulating neuronal activity patterns, synaptic plasticity, and neuronal differentiation (Chubakov et al., 1986; Gu and Singer, 1995; Cases et al., 1996; Yan et al., 1997), serotonin may play an important role during circuit development. Because spontaneous synaptic activity plays a particularly important role in shaping neuronal circuits, serotonergic modulation of intrinsic activity may represent an important mechanism regulating circuit response properties in both the adult and developing cortex. These effects can be mediated by various serotonin receptors, which are broadly subdivided into the G-protein-coupled receptors and the ionotropic 5-HT$_3$ receptor. In this study we investigated the effects of the 5-HT$_3$ receptor, which accounts for
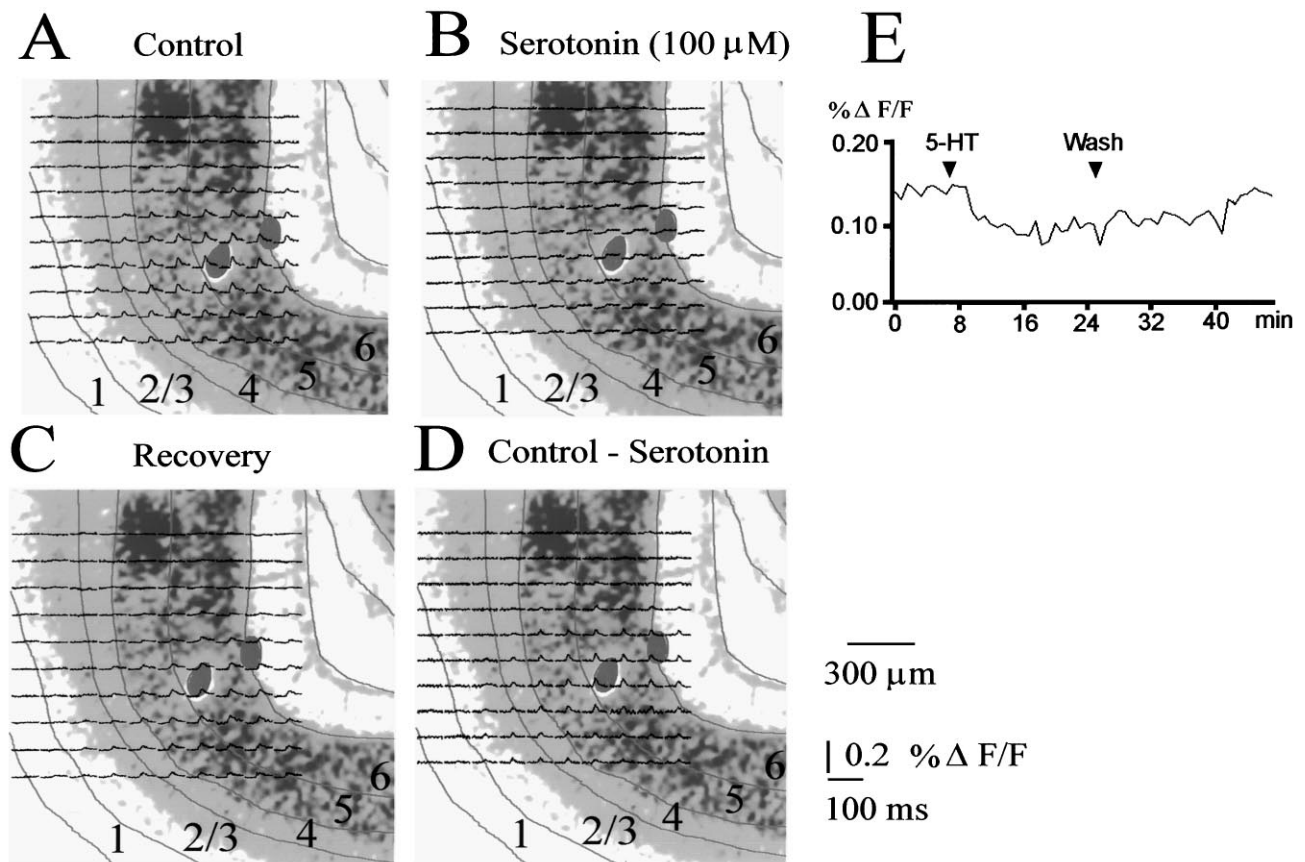
Figure 6. Reduction of response amplitudes by serotonin. *A–D*, Traces recorded from a P29 slice after stimulation in layer 6 overlaid on cresyl violet-stained sections. *Red lines* indicate laminar boundaries. Serotonin reduces in particular the fast components of the voltage-sensitive dye signal (*B*). The effect was reversible within 10–20 min; recovery traces are shown in *C*. *D* shows the difference between control responses and responses recorded in the presence of serotonin. The time course of the maximum amplitude trial by trial illustrating the inhibition induced by serotonin and its reversibility is shown in *E*.

a large part of the effects of the serotonin on cortical circuit response properties during postnatal development of the ferret visual cortex. Both optical recording and patch-clamp experiments reveal a net inhibitory effect of serotonin 5-HT$_3$ receptor stimulation on evoked synaptic responses. Optical recording provides a faithful measure of the spatiotemporal properties of neuronal activity on a circuit level (Grinvald et al., 1982, 1994; Albowitz and Kuhnt, 1993; Sutor et al., 1994; Nelson and Katz, 1995; Jackson and Scharfman, 1996; Tanifuji et al., 1996). The depression of circuit activation revealed by optical recording peaked between P32–P35 and P40–P45, which corresponds to the period of axonal cluster refinement and maturation of orientation tuning in the supragranular layers (Chapman and Stryker, 1993; Dalva and Katz, 1994; Nelson and Katz, 1995; Durack and Katz, 1996; Ruthazer and Stryker, 1996). The main mechanism underlying the circuit inhibition is likely to be activation of the GABAergic network, because on a single-cell level the predominant effect of receptor selective agonists was to increase the frequency of spontaneous GABAergic synaptic currents. This circuit effect of fast, ligand-gated serotonin receptors may represent a mechanism to modulate intracortical processing.

Ionotropic serotonin receptors modulate synaptic background activity

Spontaneous activity plays a crucial role during the periods of circuit formation that precede the maturation of sensory inputs.

Afferents from the brainstem or the basal forebrain might be involved in activity-dependent stages of cortical circuit formation by providing a source of synaptic activity and/or by regulating intracortical synaptic background activity. Spontaneous synaptic background activity alters neuronal integration properties by changing the average membrane potential and the electrotonic structure of the postsynaptic neurons (Bernander et al., 1991), which may shape activity patterns arising in the thalamocortical pathway.

Activation of 5-HT$_3$ receptors increased the frequency of GABAergic synaptic currents in the developing ferret visual cortex. In the hippocampus, 5-HT$_3$ receptors are preferentially located on interneurons where their activation increases GABAergic network activity (Kawa, 1994; McMahon and Kauer, 1995). Our results indicate that a similar mechanism might operate in the neocortex. The expression of 5-HT$_3$ receptors in neocortical neurons, especially in subpopulations of GABAergic interneurons, has been demonstrated (Tecott et al., 1993; Morales and Bloom, 1997).

An inhibitory action of the serotonergic system on thalamocortical and intracortical synaptic transmission has been observed previously in rat cortical slices (Read et al., 1994; Rhoades et al., 1994). These effects, however, were caused by a presynaptic, 5-HT1B receptor-mediated inhibition. We thus expected 5-HT1B receptor activation to also result in circuit inhibition. However, in
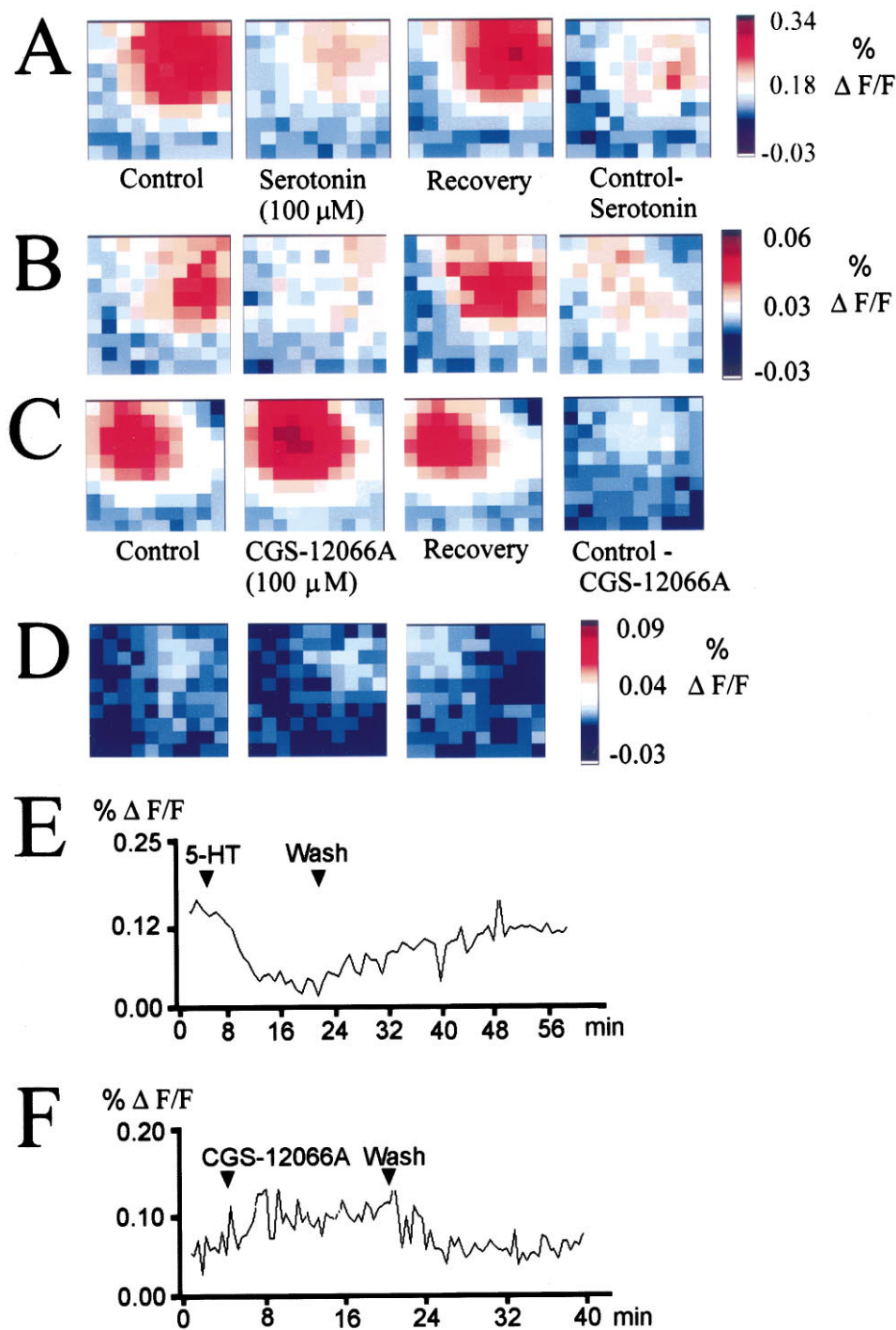
Figure 7. Maximum amplitude maps showing the effect of serotonin and the 5-HT1B agonist CGS-12066A on cortical circuit activation. *A*, Reversible suppression of circuit excitation by serotonin (100 μM) in a coronal slice from a P29 animal. The *last panel* shows the difference between the control maximum amplitude plot and the recording in the presence of serotonin. *B*, Difference plots showing the magnitude of the serotonin effect in four different slices. The stimulation electrode was placed in layer 4 (age of animals, P29–P35). *C*, Reversible excitatory effect of 5-HT1B receptor activation on circuit responses recorded in a slice from a P31 animal. The difference plot in the *last panel* represents the enhancement of circuit activation. *D*, Additional examples of the excitatory action of the 5-HT1B agonist CGS-12066A (100 μM) on cortical responses to afferent stimulation recorded from different slices (age of animals, P29–P35). *D* shows examples of difference maps obtained by subtracting the agonist-treated condition from the control response. *E, F,* Time course of serotonin and CGS-12066A action on the maximum amplitude of the cortical circuit response. Both effects were reversible.

our optical recording experiments, 5-HT1B receptor agonists increased circuit excitability. The net effect of the transmitter serotonin itself, however, was a depression of circuit activity. This is in line with our finding that most of the serotonin effect on circuit responses was mediated by 5-HT$_3$ receptors. Serotonin (5-HT) not only acts on the 5-HT$_3$ receptor but also on various G-protein-coupled receptors. Activation of these receptors might have a different effect on the cortical circuit response than 5-HT$_3$ receptor activation, as we indeed show for the 5-HT$_1$ receptor. We are therefore not surprised that the inhibitory effect of serotonin is smaller or not present in the same proportion of tested slices as the M-109 effect. We interpret our findings as the result of simultaneous activation of inhibitory and excitatory pathways by the transmitter serotonin as opposed to an exclusively inhibitory effect of 5-HT$_3$ receptor activation. It also underscores the necessity for circuit level assays to understand the effects of neuromodulators on cortical activity patterns.

Fast versus slow neuromodulator effects

How do the effects of the fast, ionotropic receptor types on circuit excitability reported here relate to known actions of the serotonergic system on cortical circuit function? The serotonin 5-HT$_3$
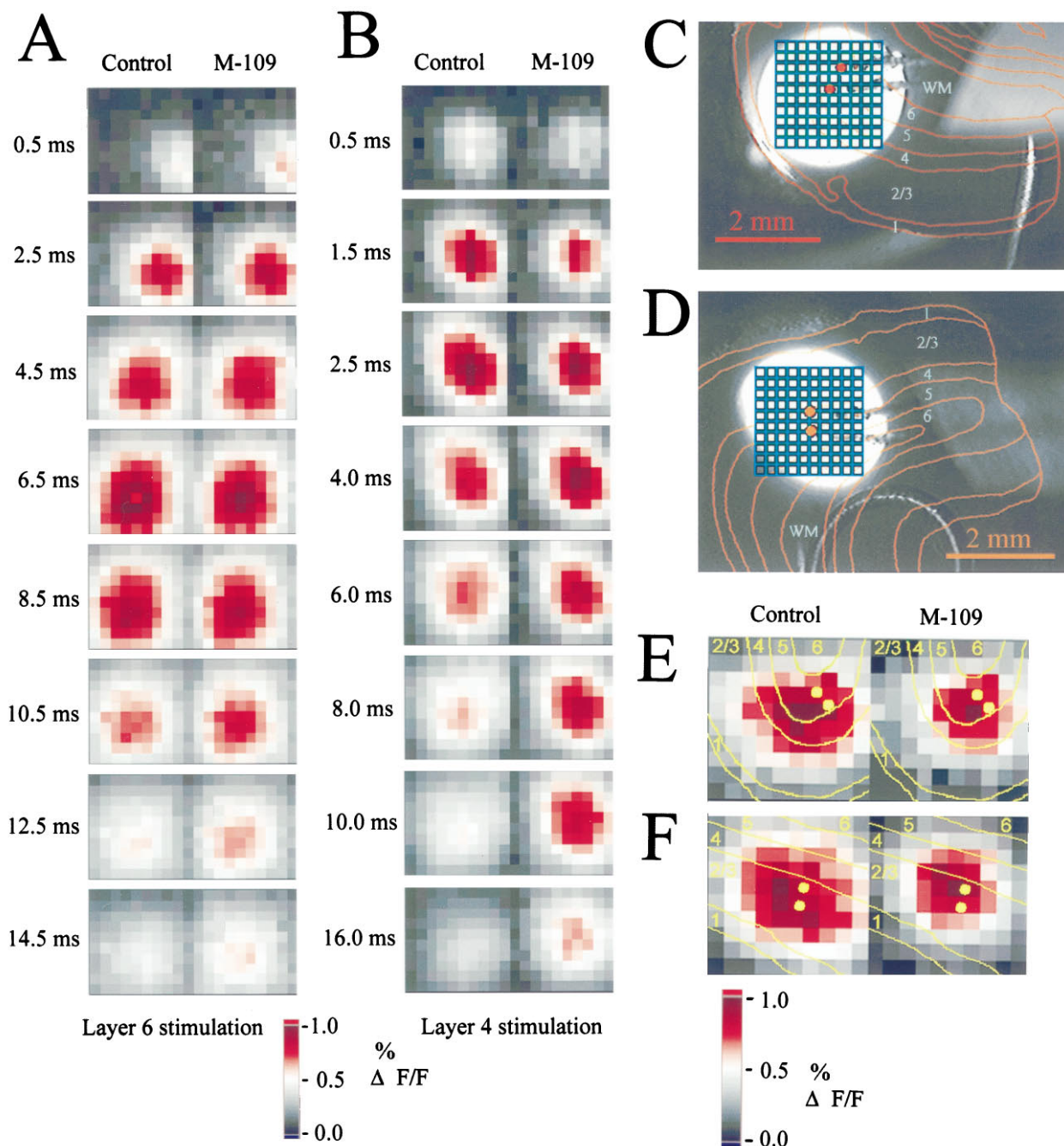
Figure 8. Effects of 5-HT$_3$ receptor activation on the time course and the spatial pattern of the cortical circuit response. Recordings shown were made in slices from a P34 animal. *A, B,* Amplitude plots of the cortical response at different times after the electrical stimulus. *A,* Stimulation in layer 6. *B,* Stimulation in layer 4. *Left panels,* Control responses; *right panels,* responses recorded in the presence of M-109 (100 μM). To emphasize the time course effect, all amplitude plots are intrinsically normalized to the maximal response in each recording; i.e., the effect of the agonist on response amplitudes is discarded here. The effect of M-109 on the signal rise was variable between slices; there was either no significant effect or a slight acceleration or prolongation of the rise time to maximal response. The signal decay was typically considerably prolonged, in particular after layer 4 stimulation (*B*). *C, D,* Video images of slices showing the illuminated area, the position of the photodiode array (*green*), and the stimulation electrode. Overlaid *red lines* represent laminar boundaries as reconstructed from cresyl violet-stained sections. *E, F,* Normalized maximum amplitude maps showing the restriction in the spatial extent of cortical activation in the presence of the 5-HT$_3$ receptor agonist. *Yellow lines* indicate laminar boundaries. Both examples are from a P44 ferret. *E,* After electrical stimulation in layer 5, the lateral extent of the activated area and the activation of the upper cortical layers is reduced. *F,* If the cortex is stimulated in layers 2/3, the lateral spread of excitation along the supragranular layers is suppressed.

receptor represents a fast acting system that is prone to desensitization. Its effect on cortical circuit activity patterns is thus very likely to be under much tighter temporal control than the effects of the slower acting, G-protein-coupled serotonin receptors. If activation of these receptors slightly precedes or temporally co-

incides with thalamic activation, the specific input encounters a cortical network that shows higher, predominantly GABAergic, synaptic background activity as compared with conditions when serotonergic inputs are silent. Because the overall consequence of this seems to be a reduction in circuit excitability, it might make
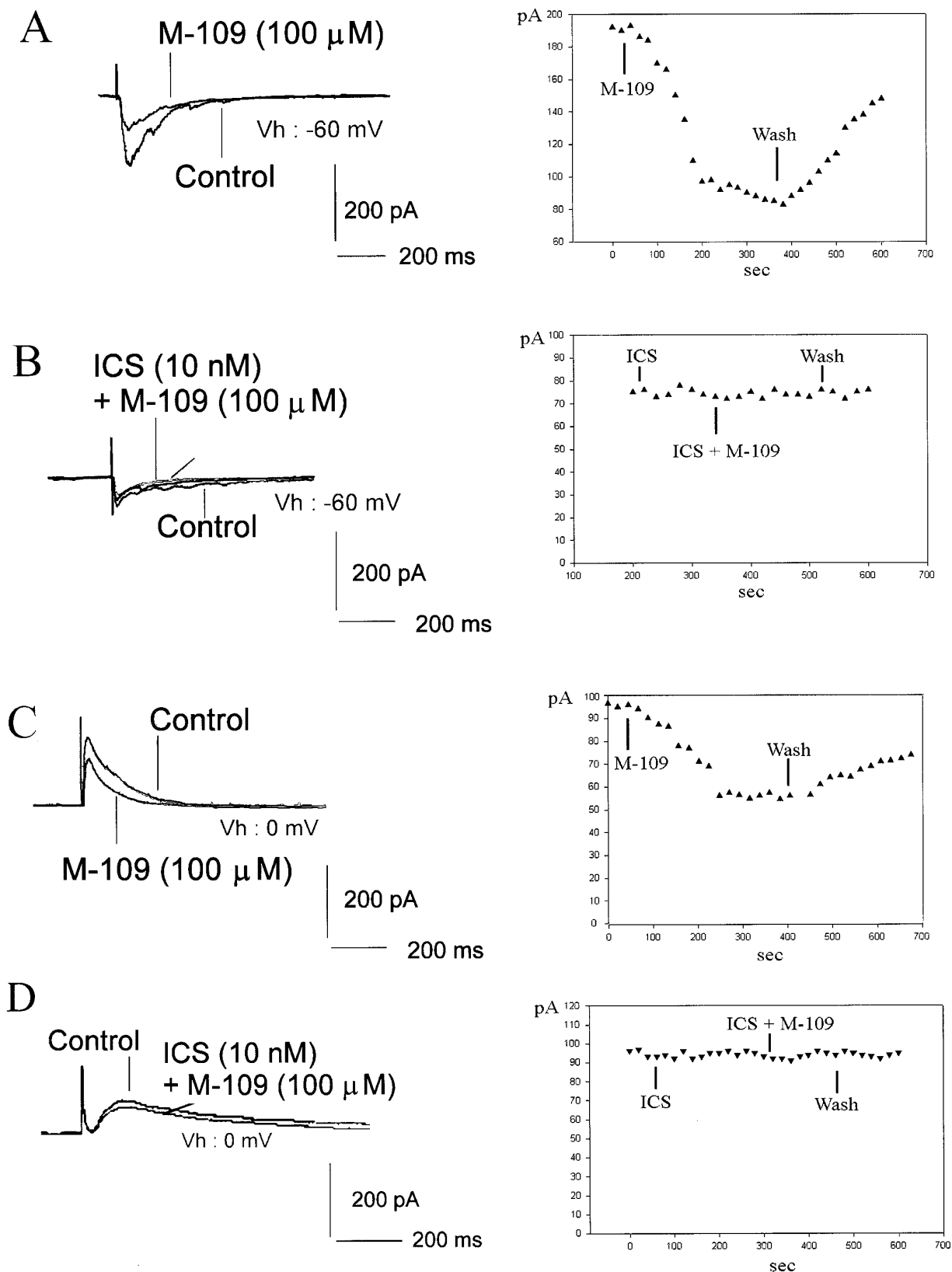
Figure 9. Effects of 5-HT$_3$ receptor on afferent-evoked synaptic responses recorded from single cells in the whole-cell patch-clamp configuration. *A, C,* The 5-HT$_3$ receptor agonist M-109 (100 μM) reduces both glutamatergic (*A*) and GABAergic (*C*) electrically evoked synaptic responses. Recordings were made from a P30 pyramidal cell (*A*) and a P36 stellate cell (*C*). *B, D,* The effect was suppressed by the 5-HT$_3$ receptor antagonist ICS 205–930 (10–20 nM; *gray traces*). Recordings from a P16 (*B*) and a P8 (*D*) pyramidal cell. All traces represent the averages of at least 20 recordings. Evoked IPSCs (*C, D*) were recorded in the presence of 20 μM D-APV and 50 μM CNQX. The *last panel* in each row shows the time course of the peak PSC amplitude measured every 20 sec.
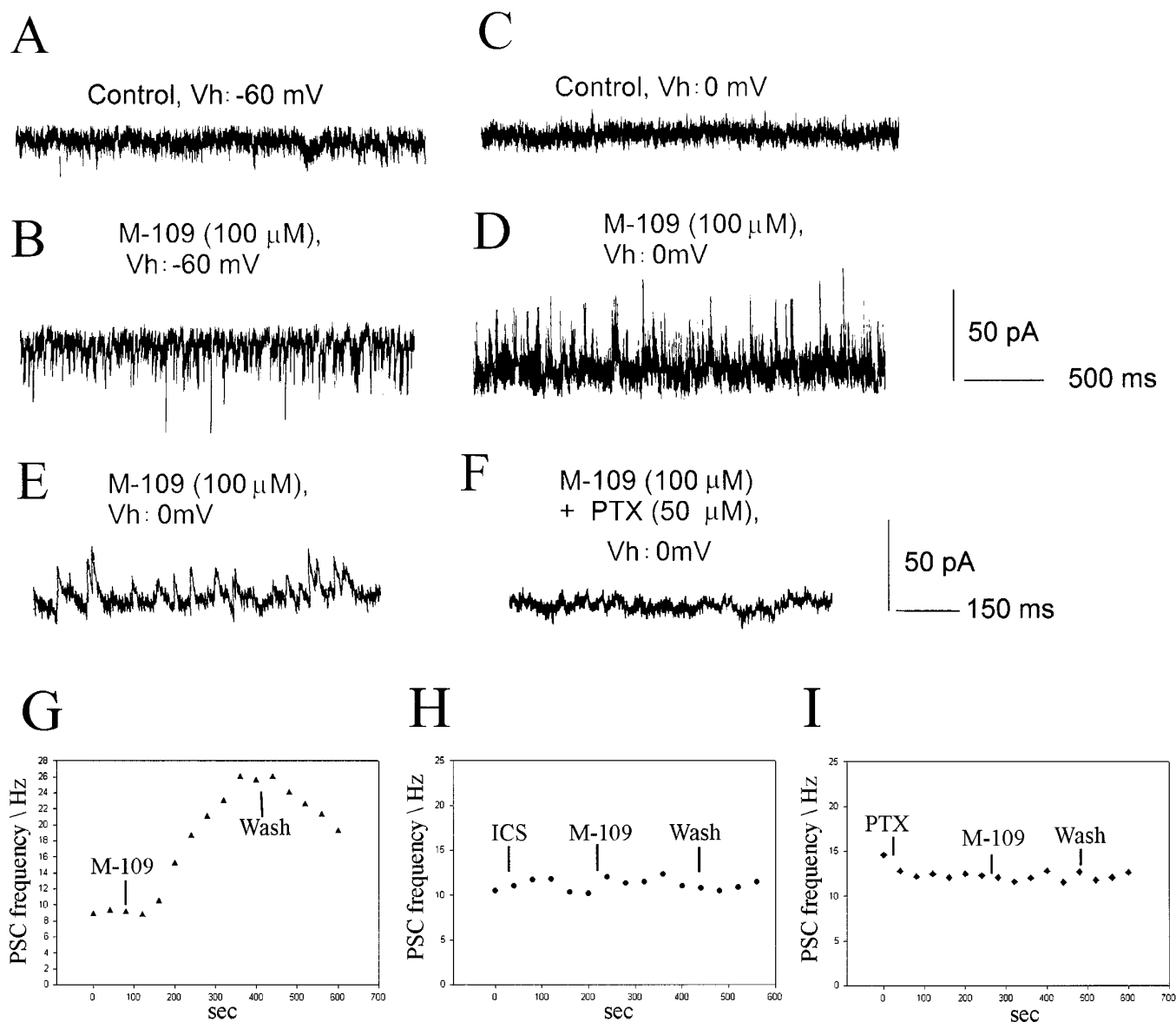
Figure 10. M-109 increases spontaneous GABAergic synaptic activity. Recordings were made from a P26 layer 2/3 pyramidal cell. *A, C,* The neuron showed no significant spontaneous synaptic activity at either -60 mV (*A*) or 0 mV (*C*) holding potential. *B,* Bath application of M-109 (100 μM) dramatically increased the frequency of spontaneous synaptic currents. *D,* The synaptic currents induced by 5-HT$_3$ receptor activation reversed around -20 mV, indicating that they were GABA$_A$ receptor-mediated. *E, F,* Recordings from the same cell shown at expanded time scale. Outward currents recorded at -20 or 0 mV were completely abolished by 50 μM picrotoxin (*F*) or 10–20 μM bicuculline, demonstrating that they were mediated by GABA$_A$ receptors. *G,* Time course of the frequency increase induced by M-109 for the cell shown in *A. H, I,* Both ICS and picrotoxin suppressed the frequency increase in GABAergic spontaneous activity induced by M-109.

the cortical substrate more selective, allowing only the strongest inputs to significantly activate the cortical circuitry. In this case, increased synaptic background activity would serve as a mechanism to enhance signal-to-noise ratios. Consistent with this, stimulation of the raphe nuclei reduces background spiking activity and evoked responses in rat prefrontal cortex (Mantz et al., 1990) and kitten visual cortex (Raevskii, 1981). The involvement of 5-HT$_3$ receptors in these effects, however, has not yet been investigated. In the hippocampus, the 5-HT$_3$ receptor-mediated increase in GABAergic network activity (Kawa, 1994) leads to decreased excitability of pyramidal cells and reduced long-term potentiation induction (Staubli and Xu, 1995; Reznic and Staubli,

1997). Our results indicate the presence of similar mechanisms in the neocortex.

In summary, our study shows an inhibitory effect of synaptic background activity induced by fast-acting serotonin-gated receptors on incoming afferent activation. Modulation of stimulus-driven responses by ongoing activity in cortical networks has been observed (Arieli et al., 1995, 1996) and may be involved in cortical computation. Our results suggest that serotonergic afferents from the raphe nuclei could pattern intracortical activity in a way that strongly affects the intracortical processing of synaptic inputs. The involvement of the fast, desensitizing receptor types indicates the capacity for tight temporal correlations between input
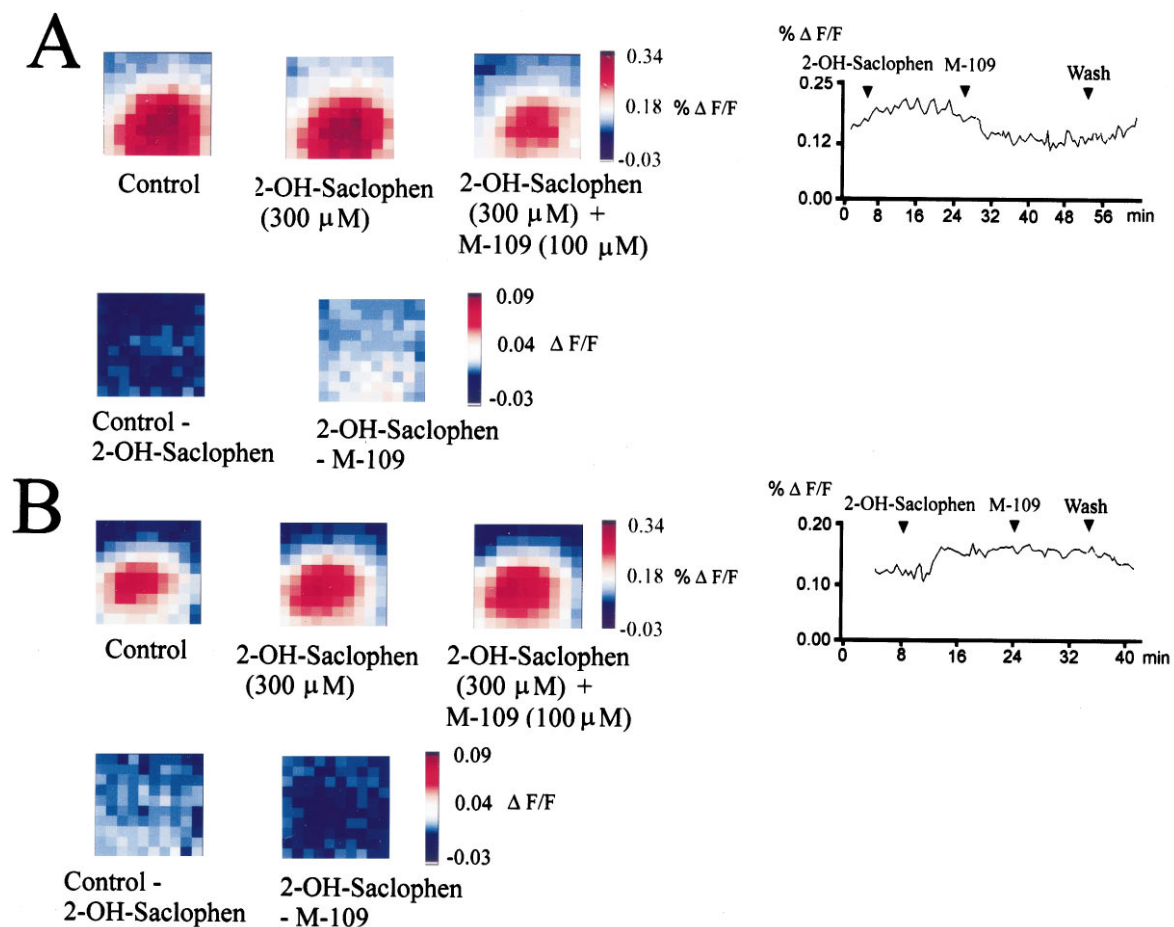
Figure 11. GABA$_B$ receptor activation contributes to the inhibitory effect of serotonin 5-HT$_3$ receptors on cortical circuit responses. *A*, *B*, Maximum amplitude maps recorded in slices from a P29 animal after electrical stimulation at the layer 6/white matter boundary. Application of the GABA$_B$ receptor antagonist 2-OH-saclophen (300 μM) slightly increased (*B*) or did not effect circuit excitation (*A*). The inhibitory action of the 5-HT$_3$ receptor agonist M-109 (100 mM) was either partially (*A*) or in some cases almost completely (*B*) antagonized by GABA$_B$ receptor blockade. The *bottom rows* show difference plots to demonstrate the size of effects more clearly. The *last panels* in the *top rows* in *A* and *B* show the time course of drug effects on the averaged maximum amplitudes (first 20 msec after stimulus onset averaged over all 100 positions per trial) and their reversibility.

systems. Because the strength of these mechanisms changes during postnatal development, they may play a role not only in mature cortical processing but also during circuit development.

REFERENCES

Aghajanian KG, Rasmussen K (1989) Intracellular studies in the facial nucleus illustrating a simple new method for obtaining viable motorneurons in adult rat brain slices. Synapse 3:331–338.

Albowitz B, Kuhnt U (1993) Evoked changes of membrane potential in guinea pig sensory neocortical slices: an analysis with voltage-sensitive dyes and a fast optical recording method. Exp Brain Res 93:213–225.

Arieli A, Shoham D, Hildesheim R, Grinvald A (1995) Coherent spatiotemporal patterns of ongoing activity revealed by real-time optical imaging coupled with single-unit recording in cat visual cortex. J Neurophysiol 73:2072–2093.

Arieli A, Sterkin A, Grinvald A, Aertsen A (1996) Dynamics of ongoing activity: explanation of the large variability in evoked cortical responses. Science 273:1868–1871.

Bear MF, Singer W (1986) Modulation of visual cortical plasticity by acetylcholine and noradrenaline. Nature 320:172–176.

Bernander O, Douglas RJ, Martin KAC, Koch C (1991) Synaptic background activity influences spatiotemporal integration in single pyramidal cells. Proc Natl Acad Sci USA 88:11569–11573.

Blanton MG, LoTurco JJ, Kriegstein AR (1989) Whole cell recording from neurons in slices of reptilian and mammalian cerebral cortex. J Neurosci Methods 30:203.

Cases O, Vitalis T, Seif I, De Maeyer E, Sotelo C, Gaspar P (1996) Lack of barrels in the somatosensory cortex of monoamine oxidase A deficient mice: role of a serotonin excess during the critical period. Neuron 16:297–307.

Chapman B, Stryker MP (1993) Development of orientation selectivity in ferret visual cortex and effects of deprivation. J Neurosci 13:5251–5262.

Chubakov AR, Gromova EA, Konovalov GV, Sarkisowa EF, Chumasov EI (1986) The effects of serotonin on the morpho-functional development of rat cerebral neocortex in tissue culture. Brain Res 369:285–297.

Dalva MB, Katz LC (1994) Rearrangements of synaptic connections in visual cortex revealed by laser photostimulation. Science 265:255–258.

D'Amato RJ, Blue ME, Largent DR, Lynch DJ, Ledbetter DJ, Molliver ME, Snyder SH (1987) Ontogeny of the serotonergic projection to rat neocortex: transient expression of a dense innervation to primary sensory areas. Proc Natl Acad Sci USA 84:4322–4326.

DeLima AD, Singer W (1986) Cholinergic innervation of the cat striate cortex: a choline acetyltransferase immunocytochemical analysis. J Comp Neurol 250:324–338.

Durack JC, Katz LC (1996) Development of horizontal projections in layer 2/3 of ferret visual cortex. Cereb Cortex 6:178–183.

Feller MB, Wellis DP, Stellwagen D, Werblin FS, Shatz CJ (1996) Requirement for cholinergic synaptic transmission in the propagation of spontaneous retinal waves. Science 272:1182–1186.

Goodman CS, Shatz CJ (1993) Developmental mechanisms that generate precise patterns of neuronal connectivity. Neuron 10[Suppl]:77–98.

Grinvald A, Manker A, Segal M (1982) Visualization of the spread of

electrical activity in rat hippocampal slices by voltage-sensitive optical probes. J Physiol (Lond) 333:269–291.

Grinvald A, Salzberg BM, Lev-Ram V, Hildesheim R (1987) Optical recording of synaptic potentials from processes of single neurons using intracellular potentiometric dyes. Biophys J 51:643–651.

Grinvald A, Lieke EE, Frostig RD, Hildesheim R (1994) Cortical point-spread function and long-range lateral interaction revealed by real-time optical imaging of macaque monkey primary visual cortex. J Neurosci 14:2545–2568.

Gu Q, Singer W (1995) Involvement of serotonin in developmental plasticity of kitten visual cortex. Eur J Neurosci 7:1146–1153.

Gu Q, Patel B, Singer W (1990) The laminar distribution and postnatal development of serotonin-immunoreactive axons in the cat primary visual cortex. Exp Brain Res 81:257–266.

Henderson Z (1991) Early development of the nucleus basalis-cortical project but late expression of its cholinergic function. Neuroscience 44:311–324.

Imamura K, Kasamatsu T (1989) Interaction of noradrenergic and cholinergic systems in regulation of ocular dominance plasticity. Neurosci Res 6:519–536.

Jackson MB, Scharfman HE (1996) Positive feedback from hilar mossy cells to granule cells in the dentate gyrus revealed by voltage-sensitive dye and microelectrode recording. J Neurophysiol 76:601–616.

Kasamatsu T, Pettigrew JD (1976) Depletion of brain catecholamines: failure of ocular dominance shift after monocular occlusion in kittens. Science 194:206–209.

Katz LC, Shatz CJ (1996) Synaptic activity and the construction of cortical circuits. Science 274:1133–1138.

Kawa K (1994) Distribution and functional properties of 5-HT$_3$ receptors in the rat hippocampal dentate gyrus: a patch-clamp study. J Neurophysiol 71:1935–1947.

Mantz J, Godbout R, Tassin JP, Glowinski J, Thierry AM (1990) Inhibition of spontaneous and evoked unit activity in the rat medial prefrontal cortex by mesencephalic raphe nuclei. Brain Res 524:22–30.

McMahon LL, Kauer JA (1995) Hippocampal s. radiatum interneurons express functional serotonin receptors. J Neurosci Abstr 1:590.

Morales M, Bloom FE (1997) The 5-HT$_3$ receptor is present in different subpopulations of GABAergic neurons in the rat telencephalon. J Neurosci 17:3157–3167.

Nelson DA, Katz LC (1995) Emergence of functional circuits in ferret visual cortex visualized by optical imaging. Neuron 15:23–34.

Raevskii VV (1981) Role of raphe nuclei in the development of somatosensory cortex neuronal activity in the kitten. Zh Vyssh Nervn Deyat Im I P Pavlova 31:349–357.

Read HL, Beck GB, Dun NJ (1994) Serotonergic suppression of inter-hemispheric cortical synaptic potentials. Brain Res 643:17–28.

Reznic J, Staubli U (1997) Effects of 5-HT$_3$ receptor antagonism on hippocampal cellular activity in the freely moving rat. J Neurophysiol 77:517–521.

Rhoades RW, Bennett-Clarke CA, Shi M-Y, Mooney RD (1994) Effects of 5-HT on thalamocortical synaptic transmission in the developing rat. J Neurophysiol 72:2438–2450.

Roerig B, Nelson DA, Katz LC (1997) Fast synaptic signaling by nicotinic acetylcholine and serotonin 5-HT$_3$ receptors in developing visual cortex. J Neurosci 17:8353–8362.

Ruthazer ES, Stryker MP (1996) The role of activity in the development of long-range horizontal connections in area 17 of the ferret. J Neurosci 16:7253–7269.

Staubli U, Xu F (1995) Effects of 5-HT$_3$ receptor antagonism on theta rhythm, memory, and LTP induction in the freely moving rat. J Neurosci 15:2445–2452.

Sugita S, Shen K-Z, North RA (1992) 5-Hydroxytryptamine is a fast excitatory transmitter at 5-HT$_3$ receptors in rat amygdala. Neuron 8:199–203.

Sutor B, Hablitz JJ (1989) EPSPs in rat neocortical neurons *in vitro*. II. Involvement of *N*-methyl-D-aspartate receptors in the generation of EPSPs. J Neurophysiol 61:621–634.

Sutor B, Hablitz JJ, Rucker F, ten Bruggencate G (1994) Spread of epileptiform activity in the immature rat neocortex studied with voltage-sensitive dyes and laser scanning microscopy. J Neurophysiol 72:1756–1768.

Tanifuji M, Yamanaka A, Sunaba R, Terakawa S, Toyama K (1996) Optical responses evoked by white matter stimulation in rat visual cortical slices and their relation to neuronal activities. Brain Res 738:83–95.

Tecott LH, Maricq AV, Julius D (1993) Nervous system distribution of the serotonin 5-HT$_3$ receptor mRNA. Proc Natl Acad Sci USA 90:1430–1434.

Thompson SM, Madison DV, Mody I (1995) Synaptic action of amino acid neurotransmitters. In: The cortical neuron (Gutnick MJ, Mody I, eds). New York: Oxford UP.

Voigt T, De Lima AD (1991b) Serotonergic innervation of the ferret cerebral cortex. II. Postnatal development. J Comp Neurol 314:415–428.

Weliky M, Katz LC (1997) Disruption of orientation tuning in visual cortex by artificially correlated neuronal activity. Nature 386:680–685.

Yan W, Wilson CC, Haring JH (1997) Effects of neonatal serotonin depletion on the development of rat dentate granule cell. Dev Brain Res 98:177–184.